Organic & Biomolecular Chemistry

Accepted Manuscript

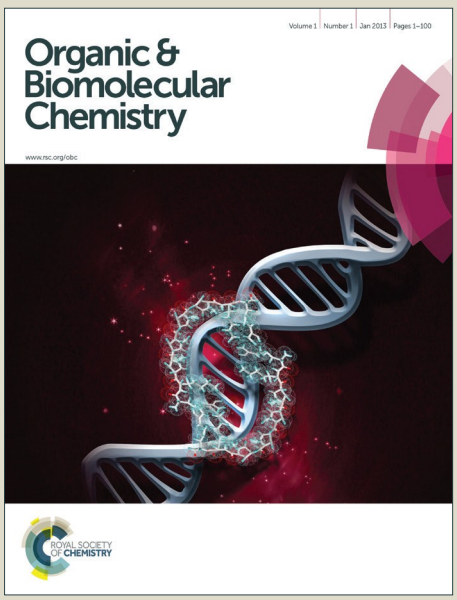

ROYAL SOCIETY OF CHEMISTRY

www.rsc.org/obc

Organic & Biomolecular Chemistry

PAPER

Docking study and biological evaluation of pyrrolidine-based iminosugars as pharmacological chaperones for Gaucher disease

Received 00th January 20xx,
Accepted 00th January 20xx

DOI: 10.1039/x0xx00000x

www.rsc.org/

Atsushi Kato,*[a] Izumi Nakagome,[b] Kasumi Sato,[a] Arisa Yamamoto,[a] Isao Adachi,[a] Robert J. Nash,[c] George W. J. Fleet,[d] Yoshihiro Natori,[e] Yasuka Watanabe,[e] Tatsushi Imahori,[e] Yuichi Yoshimura,[e] Hiroki Takahata,[e] Shuichi Hirono*[b]

We report on the synthesis and biological evaluation of a series of α-1-*C*-alkylated 1,4-dideoxy-1,4-imino-D-arabinitol (DAB) derivatives as pharmacological chaperones for Gaucher disease. The parent compound, DAB, did not show inhibition of human β-glucocerebrosidase but showed moderate intestinal α-glucosidase inhibition; in contrast, extension of α-1-*C*-alkyl chain length gave a series of highly potent and selective inhibitors of the β-glucocerebrosidase. Our design of α-1-*C*-tridecyl-DAB (**5j**) produced a potent inhibitor of the β-glucocerebrosidase, with IC_{50} value of 0.77 μM. A molecular docking study revealed that the α-1-*C*-tridecyl group has a favorable interaction with the hydrophobic pocket and the sugar analogue part (DAB) interacted with essential hydrogen bonds formed to Asp127, Glu235 and Glu340. Furthermore, α-1-*C*-tridecyl-DAB (**5j**) displayed enhancement of activity at an effective concentration 10-times lower than isofagomine. α-1-*C*-Tridecyl-DAB therefore provides the first example of a pyrrolidine iminosugar as a new class of promising pharmacological chaperones with the potential for treatment of Gaucher disease.

Introduction

Gaucher disease is caused by mutations in the *GBA1* gene encoding β-glucocerebrosidase (acid β-glucosidase, EC 3.2.1.45), responsible for the hydrolysis of glucosylceramide to ceramide and glucose.[1] The mutations of *GBA1* exhibit total or partial deficiency of β-glucocerebrosidase activity as a consequence of protein misfolding and degradation by the endoplasmic reticulum (ER) and this causes the progressive accumulation of glucosylceramide in macrophages. This abnormal metabolite eventually leads to various clinical manifestations that include hepatosplenomegaly, secondary hypersplenism, anaemia, skeletal abnormality, and neurologic dysfunction.[2] Gaucher disease has three clinical phenotypes with, differences in primary neurologic involvement and age of onset. Type I presents clinical symptoms without neuronopathic involvement. In contrast, types II and III patients have central nervous system impairment. Type I Gaucher disease is in the most common form, occurring in approximately 1 in 40,000-60,000 live births in the general population and 1 in 500-1,000 among the Ashkenazi Jewish population.[3] *GBA1* is located in chromosome 1q21. There is an adjacent pseudogene with 96% exonic sequence homology that further complicates mutation detection strategies.[4]

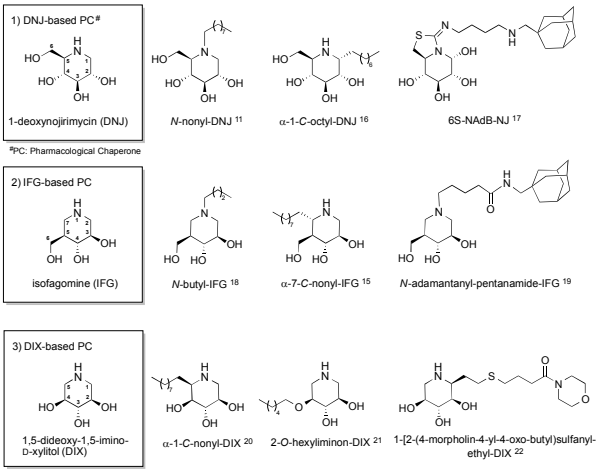

Figure 1. Structures of representative piperidine iminosugar-type GCase pharmacological chaperon.

To date, more than 200 different point mutations have been identified within the *GBA1* gene.[5] Among them, the mutation N370S is the most common genotype in the Ashkenazi Jewish population which has a less severe form of type 1 Gaucher disease. Previous studies suggested that N370S mutation

[a] Department of Hospital Pharmacy, University of Toyama, 2630 Sugitani, Toyama 930-0194, Japan; E-mail: kato@med.u-toyama.ac.jp.
[b] School of Pharmaceutical Sciences, Kitasato University, Tokyo 108-8641, Japan; E-mail: hironos@pharm.kitasato-u.ac.jp
[c] Institute of Biological, Environmental and Rural Sciences / Phytoquest Limited, Plas Gogerddan, Aberystwyth, Ceredigion, SY23 3EB, United Kingdom
[d] Chemistry Research Laboratory, Department of Chemistry, University of Oxford, Oxford, OX1 3TA, United Kingdom
[e] Faculty of Pharmaceutical Sciences, Tohoku Pharmaceutical University, Sendai 981-8558, Japan

† Footnotes relating to the title and/or authors should appear here.
Electronic Supplementary Information (ESI) available: [details of any supplementary information available should be included here]. See DOI: 10.1039/x0xx00000x

affects the α-helix 7 at the interface between the catalytic domain III and domain II and it caused an overall conformational change of β-glucocerebrosidase.[6] Thus, the mutation point is not close to the catalytic site: the mutated enzyme keeps the kinetic properties, while its thermostability is lower than the wild-type enzyme at neutral pH conditions.[7, 8] N370S mutated enzyme exhibits residual hydrolytic activity (~32%), which is higher than the other mutations G202R (~10%) and L444P (~12%).[9]

Pharmacological chaperone therapy is based on the concept that reversible competitive inhibitors assist the stabilization of the three-dimensional conformation of unstable mutated enzymes and facilitate the proper folding, thereby accelerating the mature processing and transport to the final cellular destination of the protein.[10] In order to establish the concept of using competitive inhibitors as specific pharmacological chaperones, a number of naturally occurring and chemically synthesized iminosugars were tested for intracellular enhancement of β-glucocerebrosidase activity.[2]

N-Nonyl-1-deoxynojirimycin (*N*-nonyl-DNJ : Figure 1) is an effective pharmacological chaperone for the treatment of Gaucher disease.[11] The parent iminosugar, DNJ, closely mimics the D-glucose structure. This structural similarity to D-glucose can achieve tight affinity with β-glucocerebrosidase; it is also known that these DNJ-based chaperones are potent inhibitors of ER processing α-glucosidases and intestinal digestive α-glucosidases. This non-specific α-glucosidase inhibition in various organs causes side effects such as diarrhea and impairment of liver function. Similarly, *N*-butyl-1-deoxynojirimycin (Zavesca®) with a shorter *N*-alkyl chain was launched as a potential drug for substrate reduction therapy (SRT). The basic concept of SRT is to reduce the rate of biosynthesis of glycosphingolipids to offset the catabolic defect, restoring the balance between the rate of biosynthesis and the rate of catabolism. Despite this therapeutic breakthrough, several drawbacks concerning this therapy have also been reported.[12] The most common adverse events due to Zavesca® included weight loss, diarrhea, and trembling of the hand in approximately 30% of patients; this may be because Zavesca® inhibits not only glucosyltransferase but also intestinal digestive glycosidases and ER processing α-glycosidase I and II.[13]

In phase II clinical trials it was shown that isofagomine (Plicera® : Figure 1), also a potent inhibitor of β-glucocerebrosidase *in vitro,* increases patient β-glucocerebrosidase activity without unwanted side effects;[14] however, the effects were not sufficient to significantly reduce symptoms of Gaucher disease. One of the reasons for this may be that while isofagomine has favorable van der Waals interactions and hydrogen bonding networks with β-glucocerebrosidase, it has no interactions with the hydrophobic domain.[15]

In this context, recent pharmacological chaperones for Gaucher disease belong mainly to three different pyranose sugar mimics (Figure 1): (i) 1-deoxynojirimycin (DNJ)-based pharmacological chaperones, such as *N*-nonyl-DNJ,[11] α-1-*C*-octyl-DNJ,[16] 6S-NAdB-NJ,[17] (ii) isofagomine (IFG)-based based pharmacological chaperones, such as *N*-butyl-IFG,[18] α-7-*C*-nonyl-IFG,[15] *N*-adamantyl amide IFG,[19] and (iii) 1,5-dideoxy-1,5-imino-D-xylitol (DIX)-based pharmacological chaperones, such as α-1-*C*-nonyl-DIX,[20] 2-*O*-hexyl-DIX,[21] 1-[2-(4-morpholin-4-yl-4-oxo-butyl)sulfanyl-ethyl-DIX.[22]

These pharmacological chaperones are all limited to the piperidine structures as pyranose analogues; new approaches and concepts need to be explored. Thus, we turned our attention to the design of pyrrolidine-based pharmacological chaperones. It is not usually easy to predict the glycosidase inhibition profiles of polyhydroxylated pyrrolidine alkaloids based on the configuration of the hydroxyl groups.[23] For the rational drug design of clinically available pharmacological chaperones, we first reported the synthesis from the enantiomers of glucuronolactone of all 10 stereoisomeric 2,5-dideoxy-2,5-iminohexitols.[24] A side-by-side comparison showed that 8 of the 10 stereoisomers gave significant inhibition of varying glycosidases. On the basis of these preliminary studies, we prepared 1,4-dideoxy-1,4-imino-D-arabinitol (DAB) with different alkyl chain lengths. In particular, we have investigated the effect of the configuration of the hydroxyl groups on the pyrrolidine ring and alkyl chain length on the stabilization of β-glucocerebrosidase under heat-shock conditions and pharmacological chaperone effects against N370S Gaucher fibroblasts.

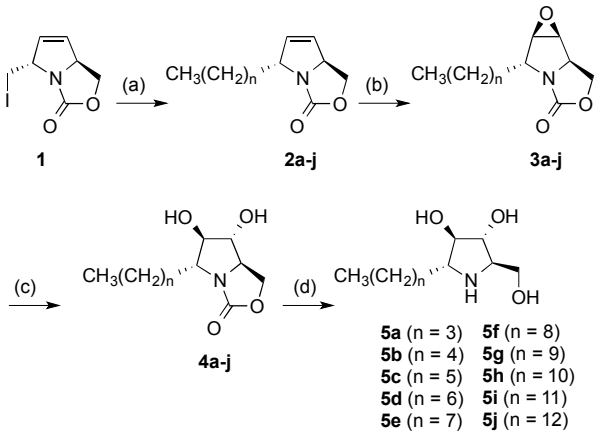

Scheme 1. Synthesis of α-1-*C*-alkyl-DAB. Reagents: (a) alkylzinc bromide (3.2 eq.), $Ni(cod)_2$ (16 mol%), (*R*,*R*)-2,6-bis(4-isopropyl-2-oxazolin-2-yl)pyridine (32 mol%), *N*,*N*-dimethylacetamide, rt, 20 h (b) Oxone™ (5.0 eq.), CF_3COCH_3 (10.0 eq.), $NaHCO_3$ (7.5 eq.), 0 °C, 2 h (c) CF_3CO_2H (12.0 eq.), THF/H_2O (3:2), reflux, 72 h (d) NaOH (10 eq.), $EtOH/H_2O$ (2:1), reflux, 1 h.

Results and discussion

Chemistry

We previously reported the synthesis of α-1-*C*-alkyl-LABs[25] and -DABs **5a** and **5e**[26]. By similar procedures, α-1-*C*-alkyl-DABs **5a-j** with various lengths of side chains from C4 to C13 at the 1-position were synthesized. A chiral common intermediate **1**[25, 26] was subjected to the Negishi coupling reaction with alkylzinc bromides to afford coupled products **2a-j** in 57-89% yields. Epoxidation of **2a-j** with trifluorodimethyldioxirane, generated

by the treatment of trifluoroacetone and Oxone™, gave epoxides **3a-j** as single diastereomers in good yields. As we reported in previous studies, the steric bulk of a C1 substituent ensured that highly diastereoselective addition occurred from the α-side of the dihydropyrrole ring.[25, 26] Cleavage of the oxirane ring of **3a-j** under acidic conditions afforded *trans*-diols **4a-j** which were further treated with sodium hydroxide in aqueous ethanol to give the desired α-1-*C*-alkyl-DABs **5a-j** in 46-90% yields (Scheme 1).

Influence of α-1-*C*-alkylation toward LAB and DAB as glycosidase inhibitors

We first compared α-1-*C*-alkylated LAB and DAB analogues. Our design strategy was based on experience gained in our previous studies on α-1-*C*-butyl-LAB[26] and L-isoDMDP[27]. These pyrrolidine derivatives were designed as selective inhibitors of intestinal α-glucosidases; they showed a strong and early-phase suppression of postprandial hyperglycemia with an effective dose 10-times lower than that for miglitol, a drug presently used in the treatment of late onset diabetes. Furthermore, we also showed that the introduction of a butyl chain at C-1 of LAB to give α-1-*C*-butyl-LAB dramatically improved its inhibitory potency against maltase and sucrase, whereas introduction of an *N*-butyl substituent into LAB reduced effectiveness as a glycosidase inhibitor.

Table 1. Concentration of α-1-*C*-alkyl-LAB and DAB derivatives giving 50 % inhibition of rat intestinal maltase, sucrase, and human β-glucocerebrosidase.

	IC_{50} (μM)					
	LAB derivatives			DAB derivatives		
	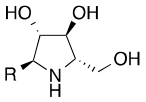			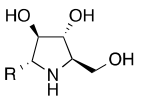		
	R=			R=		
Enzyme	H	C_4H_9	C_8H_{17}	H	C_4H_9	C_8H_{17}
α-Glucosidase						
Rat intestinal maltase	0.93[a]	0.13[a]	0.32[a]	55	NI	500
Rat intestinal sucrase	1.0[a]	0.032[a]	0.45[a]	16	393	590
β-Glucosidase						
Human β-glucocerebrosidase	NI[b]	NI	NI	NI[b]	NI	6.2

[a] Our previous data (Kato et al., *J. Med. Chem*. **55**, 10347-10362)

[b] NI : No inhibition (less than 50% inhibition at 1000 μM).

Table 1 shows the 50% inhibitory concentrations (IC_{50}) of α-1-*C*-alkyl-DAB and LAB against rat intestinal maltase, sucrase, and human β-glucocerebrosidase. The parent compound, DAB was a much weaker inhibitor of rat intestinal maltase and sucrase inhibitor than LAB. Furthermore, it is noteworthy that both DAB and LAB itself did not show inhibitory activity against human β-glucocerebrosidase. The introduction of a butyl chain at C-1 position of DAB reduced their effectiveness as rat intestinal α-glucosidase inhibitors, while it was still inactive against human β-glucocerebrosidase. In sharp contrast, α-1-*C*-octyl-DAB showed good inhibitory potency against β-glucocerebrosidase, with an IC_{50} value of 6.2 μM. This behaviour could not be observed in α-1-*C*-octyl-LAB. These results indicated that the addition of an alkyl chain to the C-1 of DAB might lead to the production of a highly potent and selective inhibitor of human β-glucocerebrosidase. Thus, we focused on the anomeric position and whether extension of the alkyl chain at this position could influence the inhibition characteristics of DAB. α-1-*C*-Butyl-DAB (**5a**) had no effect against this enzyme, whereas α-1-*C*-pentyl-DAB (**5b**) showed moderate inhibitory activity, with IC_{50} value of 34 μM (Table 2).

Table 2. IC_{50} values (μM) for α-1-*C*-alkyl-DAB (**5a-5j**) against human β-glucocerebrosidase.

Compounds	IC_{50} (μM) β-Glucocerebrosidase
α-1-*C*-Butyl-DAB (**5a**)	NI[a]
α-1-*C*-Pentyl-DAB (**5b**)	34
α-1-*C*-Hexyl-DAB (**5c**)	30
α-1-*C*-Heptyl-DAB (**5d**)	38
α-1-*C*-Octyl-DAB (**5e**)	6.2
α-1-*C*-Nonyl-DAB (**5f**)	3.3
α-1-*C*-Decyl-DAB (**5g**)	1.9
α-1-*C*-Undecyl-DAB (**5h**)	2.3
α-1-*C*-Dodecyl-DAB (**5i**)	1.5
α-1-*C*-Tridecyl-DAB (**5j**)	0.77

[a] NI : less than 50% inhibition at 1000 μM.

Further extension of the length of the α-1-*C*-alkyl chain improved the inhibition potency accordingly (**5c**-**5j**). The most potent inhibitor α-1-*C*-tridecyl-DAB (**5j**) displayed a remarkable IC_{50} value of 0.77 μM, which is 44-fold more potent relative to α-1-*C*-pentyl-DAB (**5b**). These results clearly indicate that a much longer alkyl chain than butyl is required for achieving strong inhibition of β-glucocerebrosidase. However, it is noteworthy that their inhibitory potency did not show linear characteristics but increased stepwise as shown in Figure 2.

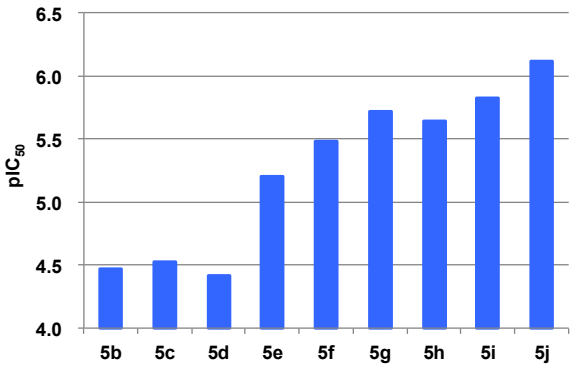

Figure 2. Representation of pIC_{50} for α-1-*C*-alkyl-DAB (**5b**-**5j**) against human β-glucocerebrosidase as a bar graph.

In vitro stabilization effect of α-1-*C*-alkyl-DAB against heat-shock β-glucocerebrosidase.

We next investigated the effect of these compounds on the stabilization of this enzyme at 45˚C (Figure 3). The enzyme β-

glucocerebrosidase was incubated in 100 mM McIlvaine buffer (pH 5.2) containing 0.25% sodium taurocholate and 0.1% Triton X-100 for 0, 20, 40 and 60 min and the remaining enzyme activity was determined with 4-methylumbellifery-β-D-glucopyranoside as substrate. Isofagomine was used as positive control. The enzyme activity was lost within 60 min under incubation without test samples (2.3% activity remained at 60 min), while the enzyme activity remained over 60% even after incubation for 60 min in the presence of 10 μM isofagomine (Figure 3). Whereas 10 μM α-1-*C*-nonyl-DAB (**5f**) tended to slightly protect the enzyme from heat stress (6.5% activity remained at 60 min), the stabilization effect was much weaker than α-1-*C*-tridecyl-DAB (**5j**). α-1-*C*-Tridecyl-DAB (**5j**) was the most efficient compound in this test, achieving 56 and 40% β-glucocerebrosidase protection after 20 and 40 min at 10 μM, respectively. These results suggested that extension of the α-1-*C*-alkyl chain length contributed to the thermostabilizing effects.

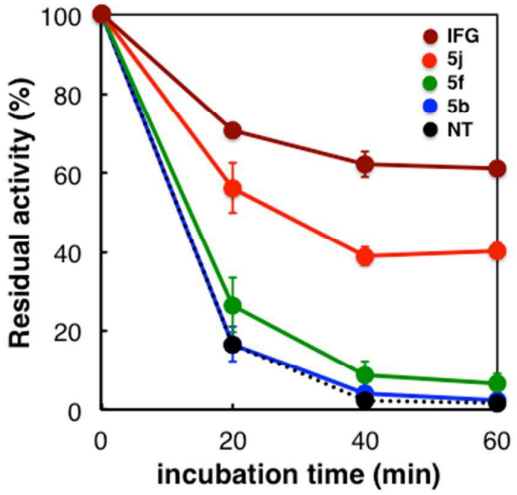

Figure 3. Effect of α-1-C-alkyl-DAB (10 μM) on the *in vitro* thermostability. The enzyme β-glucocerebrosidase was incubated at 45 ˚C in 100 mM McIlvaine buffer (pH 5.2) containing 0.25% sodium taurocholate and 0.1% Triton X-100 for 0, 20, 40, and 60 min. After incubation with isofagomine (IFG), α-1-*C*-pentyl-DAB (**5b**), α-1-*C*-nonyl-DAB (**5f**), and α-1-*C*-tridecyl-DAB (**5j**), and then the remaining β-glucocerebrosidase activity was assayed immediately using 3 mM 4-methylumbelliferl-β-D-glucopyranoside as substrate. Each value represents the mean ± SEM (n=3).

Intracellular enhancement of residual enzyme activity in human N370S fibroblasts by α-1-*C*-alkyl-DAB

We next evaluated the chaperone activity of α-1-*C*-alkyl-DAB *in vitro* in fibroblasts from a Gaucher patient with the N307S mutation. Cells were cultured in the presence of α-1-*C*-heptyl-DAB (**5b**: 25-100 μM), α-1-*C*-nonyl-DAB (**5f:** 1.0-5.0 μM), and α-1-*C*-tridecyl-DAB (**5j**: 0.25-1.0 μM) for 6 days, and the intracellular enzyme activities were determined with 4-methylumbelliferyl β-glucoside as substrate (Figure 4). Isofagomine (5 μM), which is under Phase II clinical trial toward Gaucher disease, was used as a positive control. Relative to non-treated (NT), α-1-*C*-heptyl-DAB (**5b**) improved intracellular β-glucocerebrosidase activities in N370S fibroblasts, with increases of 1.6-1.7-fold with optimal concentrations of 100 μM. α-1-*C*-Nonyl-DAB (**5f**) was also assayed under the same conditions and was effective as a pharmacological chaperone at a lower dose than α-1-*C*-heptyl-DAB (**5b**). The concentration range of achieving maximum activity enhancement was clearly lower than that of α-1-*C*-heptyl-DAB (**5b**). It is noteworthy that, α-1-*C*-tridecyl-DAB (**5j**) displayed comparable enhancement of activity to that obtained with isofagomine but at an effective concentration which was 10-times lower than isofagomine. These apparent differences between the enzyme affinities and/or enzyme stabilization effects by using naked enzyme and mutant β-glucocerebrosidase activity enhancement assay in N370S Gaucher fibroblasts could be attributed to differential penetration of the cells or organelles by isofagomine and α-1-*C*-tridecyl-DAB (**5j**). These results clearly suggested that hydrophobic side-chain derivative, such as α-1-*C*-tridecyl-, would assist in the cell-membrane-penetration of the inhibitor and contribute to its recognition in the hydrophobic pocket of β-glucocerebrosidase. Therefore, the correlation between the enzyme affinities and mutant enzyme enhancement activities in mutant Gaucher's cell could be used to estimate how well the inhibitor is able to reach an intracellular therapeutic target.

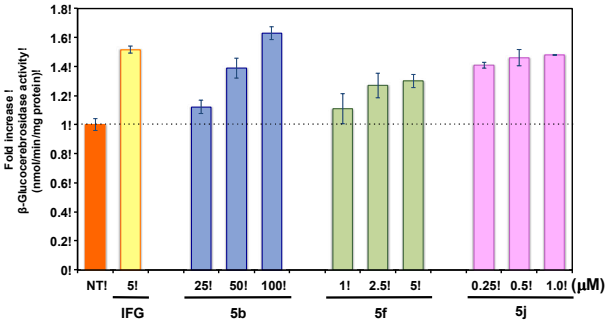

Figure 4. Effect of α-1-*C*-alkyl-DAB (**5b**, **5f**, and **5j**) on N370S GCase in Gaucher cells treated with increasing concentrations of **5a**, **5f**, or **5j**. Each value represents the mean ± SEM (n=3).

In vitro normalization effect of α-1-*C*-alkyl-DAB against cellular trafficking of the N370S mutant.

On the basis of these findings, it is clear that α-1-*C*-alkyl-DAB (**5b**, **5f**, and **5j**) led to the stabilization of mutant β-glucocerebrosidase structure and consequently increased the intracellular activity. Thus, we next focused on the subcellular localization and whether these iminosugars could improve the transport and subcellular distribution of the mutant β-glucocerebrosidase. Gaucher patient fibroblasts were incubated in the presence or absence of 100 μM α-1-*C*-pentyl-DAB (**5b:** Figure 5 D-F) or 10 μM α-1-*C*-nonyl-DAB (**5f:** Figure 5 G-I) or 1.0 μM α-1-*C*-tridecyl-DAB (**5j:** Figure 5 J-L) for 6 days. The subcellular location of β-glucocerebrosidase was then determined by double immunofluorescence analysis. Compared with no treatment (Figure 5 A), treatment with 1.0 μM α-1-*C*-tridecyl-DAB (**5j**) resulted in increase in the intensity

of GCase fluorescence throughout the cells (Figure 5 J). Furthermore, it is different from the non-treated cells (Figure 5 A-C) where the GCase staining pattern showed substantially overlap with that for lysosomal marker LAMP-1 (Figure 5 J-L). These results clearly indicated that α-1-*C*-tridecyl-DAB (**5j**) improved the subcellular trafficking and distribution of mutant enzyme.

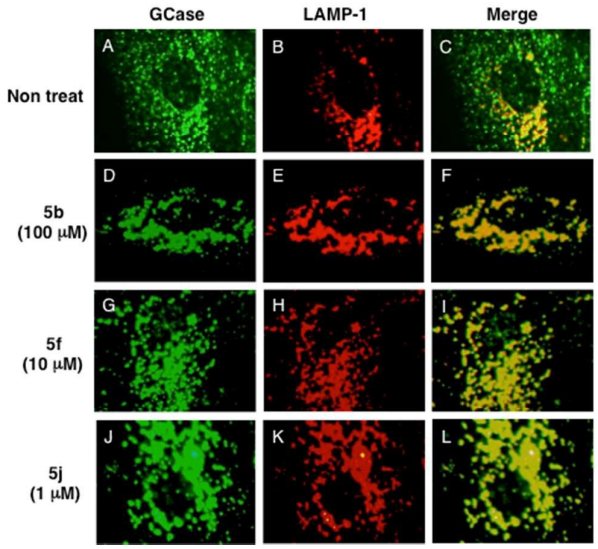

Figure 5. Immunocytochemistry of glucocerebrosidase (Gcase) in N370S Gaucher fibroblasts treated with α-1-*C*-alkyl-DAB (**5b**, **5f**, and **5j**). N370S Gaucher fibroblasts were cultured with or without 100 μM α-1-*C*-pentyl-DAB (**5b**), 10 μM α-1-*C*-nonyl-DAB (**5f**), and 1.0 μM α-1-*C*-tridecyl-DAB (**5j**) for 6 days. Immunocytochemistry was performed in which cells were double labeled with GCase antibody (green), and a lysosome marker (LAMP-1, red).

Docking study of α-1-*C*-tridecyl-DAB (5j) to human β-glucocerebrosidase

To understand the structural basis of the interaction of α-1-*C*-tridecyl-DAB (**5j**) with human lysosomal β-glucocerebrosidase, we first determined the mode of inhibition and the inhibition constant (*Ki*) from Lineweaver-Burk plots. As a result, α-1-*C*-tridecyl-DAB (**5j**) inhibited β-glucocerebrosidase in a competitive manner, with K_i value of 0.71 μM. This result suggests that α-1-*C*-tridecyl-DAB (**5j**) occupied the active-site of this enzyme in much the same way as isofagomine. In order to investigate the interaction between β-glucocerebrosidase and α-1-*C*-tridecyl-DAB (**5j**), we constructed the three-dimensional structure of the β-glucocerebrosidase-α-1-*C*-tridecyl-DAB (**5j**) complex using Induced Fit Docking protocol (See experimental section: docking studies). As shown in Figure 6, the pyrrolidine group of α-1-*C*-tridecyl-DAB (**5j**) was found to bind to the same pocket as the piperidine group of isofagomine in the crystal structure in complex with β-glucocerebrosidase (pdb_2NSX). The pyrrolidine group of α-1-*C*-tridecyl-DAB (**5j**) had favorable van der Waals interactions with Tyr313 and Trp381 of β-glucocerebrosidase. These van der Waals interactions were similar to that of the piperidine group of isofagomine. The positive nitrogen and the hydroxyl groups of α-1-*C*-tridecyl-DAB (**5j**) formed hydrogen bonding with Glu235, Glu340, Asp127 and Trp179 in β-glucocerebrosidase. We have previously reported that the ionic hydrogen bonds to Glu235 and Glu340 and non-ionic hydrogen bond to Asp127 are essential for the ligand binding with β-glucocerebrosidase.[28]

Figure 6. *Panel A and C* show the binding modes of α-1-*C*-tridecyl-DAB (**5j**) (A) and isofagomine (C) (pdb code 2NSX) with human β-glucocerebrosidase. The residues related to van der Waals interactions are drawn in space-filling representation. The hydrogen bonds are depicted by dashed lines. *Panel B and D* show the schematic diagram of hydrogen bonding interactions and vdW interactions of α-1-*C*-tridecyl-DAB (**5j**) (B) and isofagomine (D) with human β-glucocerebrosidase.

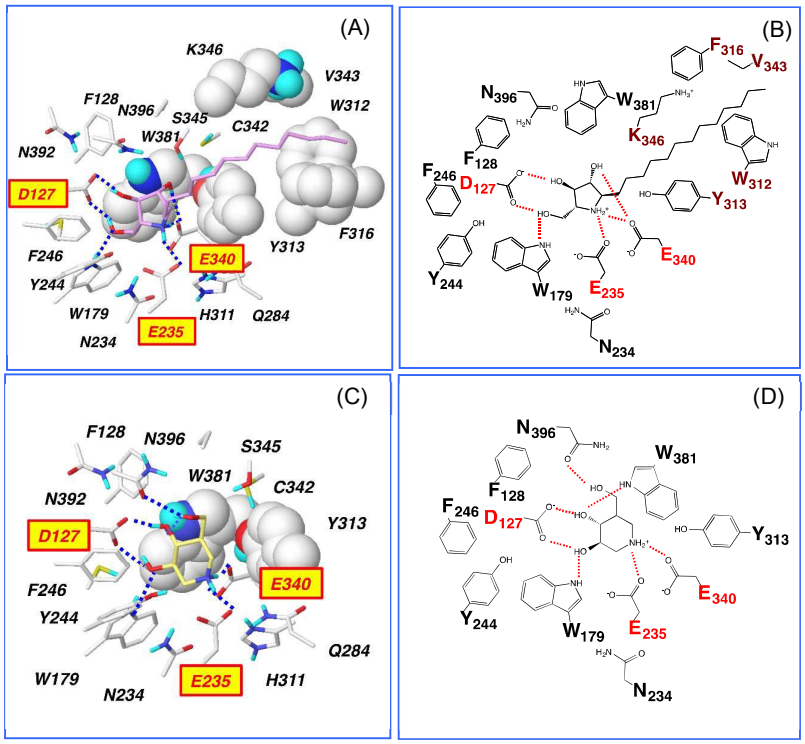

Thus, α-1-*C*-tridecyl-DAB (**5j**) has the favorable hydrogen bonding network with β-glucocerebrosidase in the same as with isofagomine. It is noteworthy that the tridecyl group of α-1-*C*-tridecyl-DAB (**5j**) is located in the long hydrophobic pocket of Trp312, Tyr313, Phe316, Val343 and the alkyl side chain of Lys346 and forming a favorable hydrophobic interaction (Figure 7). The target enzyme β-glucocerebrosidase is responsible for the cleavage of the β-glycosidic bond of glucosylceramide to release ceramide and glucose. The active site, therefore, is considered to be comprised of sites to accommodate both the sugar part "glucose" and also the hydrophobic part "ceramide". In this study, we demonstrated that α-1-*C*-butyl-DAB (**5a**) had no effect against this enzyme, whereas α-1-*C*-pentyl-DAB (**5b**) showed moderate inhibition, with IC_{50} value of 34 μM (Table 2). Furthermore, the inhibition potency was improved by extension of the α-1-*C*-alkyl chain length (**5c**-**5j**). These results suggested that the α-1-*C*-tridecyl group of α-1-*C*-tridecyl-DAB (**5j**) might be recognized by the hydrophobic pocket and thereby stabilized the favorable pyrrolidine-ring orientation, finally leading to an increase in inhibitory activity.

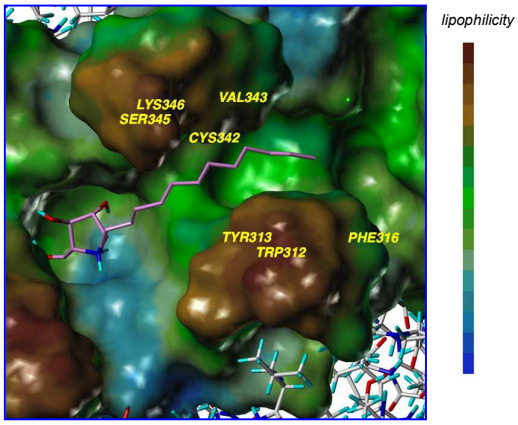

Figure 7. The binding of α-1-*C*-tridecyl-DAB (**5j**) in the active site of β-glucocerebrosidase. The molecular surface of β-glucocerebrosidase was rendered by lipophilic potential using SYBYL-X 2.0 software (Certara USA, Inc.).

Conclusion

It is clear from this study that pyrrolidine iminosugars provide a new class of pharmacological chaperones; all previously reported pharmacological chaperones have been based on piperidine structures. The present work elucidated the following features: (a) α-1-*C*-tridecyl-DAB showed the most potent inhibitory activity toward human β-glucocerebrosidase, with an IC_{50} value of 0.77 μM; (b) the parent compound, DAB, did not show any inhibition, whereas addition of an alkyl chain at the C-1 of DAB led to the production of a highly potent and selective inhibition. Extension of the α-1-*C*-alkyl chain length improved the inhibition potency. A greater length chain than butyl is required for significant inhibition; (c) the pyrrolidine group of α-1-*C*-tridecyl-DAB has favorable van der Waals interactions (Tyr313 and Trp381) and hydrogen bonding network (Glu235, Glu340, Asp127 and Trp179) with β-glucocerebrosidase. The α-1-*C*-tridecyl group of α-1-*C*-tridecyl-DAB occupies the hydrophobic pocket (Trp312, Tyr313, Phe316, Val343 and Lys346); (d) α-1-*C*-tridecyl-DAB improved the thermostability of β-glucocerebrosidase *in vitro* and displayed comparable enhancement of activity at a concentration 10-times lower than isofagomine. α-1-*C*-Tridecyl-DAB therefore represents a new class of potential pharmacological chaperones with potential for the treatment of Gaucher disease.

Experimental Section

General experimental procedures

Infrared (IR) spectra were recorded on a Perkin-Elmer 1600 series FT-IR spectrometer. Mass spectra (MS) were recorded on a JEOL JMN-DX 303/JMA-DA 5000 spectrometer. Microanalyses were performed on a Perkin-Elmer CHN 2400 Elemental Analyzer. Optical rotations were measured with a JASCO DIP-360 or JASCO P-1020 digital polarimeter. Proton nuclear magnetic resonance (^{1}H NMR) spectra were recorded on JEOL JNM-AL 400 (400 MHz) spectrometer, using tetramethylsilane as an internal standard. The following abbreviations are used: s = singlet, d = doublet, t = triplet, q = quartet, m = multiplet, br = broad. Column chromatography was carried out on Merck Silica gel 60 (230-400 mesh) or KANTO Silica Gel 60N (40-50 mm) for flash chromatography.

(*5S,7aS*)-5-(Iodomethyl)-1,7a-dihydropyrrolo[1,2-c]oxazol-3(5*H*)-one (1).

The iodide **1** was prepared according to reported procedure.[25, 26] $[\alpha]_D^{24}$ = -131.7 (*c* 1.04, $CHCl_3$). *Lit. ent*-**1** : $[\alpha]_D^{23}$= +141.6 (*c* 1.0, $CHCl_3$,).[25]

Typical procedure for the preparation of alkylzinc bromide

Iodine chips (127 mg, 0.50 mmol) were added to a suspension of Zn powder (981 mg, 15.0 mmol) in *N*,*N*-dimethylacetamide (10 mL) at room temperature. After stirring for 10 min, the resulting mixture changed from a dark-brown suspension to a colorless suspension. Alkylbromide (10 mmol) was added by syringe, and the reaction mixture was stirred at 80 °C for 3 h. The concentration in *N*,*N*-dimethylacetamide was ~0.75 M.

Typical Procedure for Negishi Coupling

Yellow bis(1,5-cyclooctadiene)nickel(0) (83.1 mg, 0.302 mmol, 16 mol %) and (*R*,*R*)-2,6-bis(4-isopropyl-2-oxazolin-2-yl)pyridine (182 mg, 0.604 mmol, 32 mol %) were added to *N*,*N*-dimethylacetamide (12.0 mL) under an argon atmosphere, and the resulting mixture was stirred for 30 min at room temperature. The resulting deep-blue solution was added to a solution of the alkylzinc bromide (in *N*,*N*-dimethylacetamide, 8.7 mL, 6.05 mmol) and **1** (500 mg, 1.89 mmol). After being

stirred for 20 h, the reaction was quenched with iodine chips (440 mg). After being stirred for 10 min, the dark-brown mixture was passed through a short pad of silica gel (eluting with AcOEt/hexane = 1/1) (to remove *N*,*N*-dimethylacetamide, inorganic salts, and iodine). The filtrate was then concentrated, and the residue was purified by flash chromatography (silica gel eluting with hexane/EtOAc) to provide coupled products **2a-j**. Compounds **2a-h** were identical in ^{1}H-NMR with *ent*-**2a-h** which were reported previously.[26]

(5*R*,7a*S*)-5-Dodecyl-1,7a-dihydropyrrolo[1,2-c]oxazol-3(5*H*)-one (2i).

60% yield; ^{1}H-NMR (400 MHz, $CDCl_3$) δ: 0.88 (3H, t, *J* = 6.8 Hz,), 1.26-1.56 (22H, m), 4.22 (1H, dd, *J* = 5.8, 8.2 Hz), 4.53 (1H, brs), 4.60 (1H, t, *J* = 8.7 Hz), 4.74 (1H, brs), 5.83-5.85 (1H, m), 6.03 (1H, ddd, *J* = 2.4, 2.4, 6.3 Hz). ^{13}C-NMR (100 MHz, $CDCl_3$) δ: 14.08, 22.64, 26.19, 29.31, 29.41, 29.49, 29.54, 29.60, 29.62, 31.87, 34.38, 63.84, 67.47, 68.71, 127.96, 135.27, 162.97. IR (neat) cm^{-1} : 1743, 2851, 2917. EI-MS (m/z) : 293 (M^+). HRMS Calcd. for $C_{18}H_{31}NO_2$: 293.2355, Found: 293.2354. $[\alpha]_D^{26}$= -124.8 (*c* 0.15, $CHCl_3$).

(5*R*,7a*S*)-5-Tridecyl-1,7a-dihydropyrrolo[1,2-c]oxazol-3(5*H*)-one (2j).

60% yield; ^{1}H-NMR (400 MHz, $CDCl_3$) δ: 0.88 (3H, t, *J* = 6.3 Hz), 1.26-1.54 (24H, m), 4,22 (1H, dd, *J* = 5.3, 8.7 Hz), 4.53 (1H, brs), 4.60 (1H, t, *J* = 8.7 Hz), 4.74 (1H, m), 5.85(1H, dd, *J* = 1.4, 5.8 Hz), 6.03 (1H, ddd, *J* = 2.4, 2.4, 6.2 Hz). ^{13}C-NMR (100 MHz, $CDCl_3$) δ: 14.08, 22.64, 26.19, 29.32, 29.41, 29.50, 29.54, 29.60, 29.62, 29.64, 31.87, 34.39, 63.84, 67.47, 68.71, 127.97, 135.27, 162.98. IR (neat) cm^{-1} : 1745, 2849, 2917. EI-MS (m/z) : 307 (M^+). HRMS Calcd. for $C_{19}H_{33}NO_2$: 307.2511, Found : 307.2519, $[\alpha]_D^{17}$= -107.9 (*c* 0.52, $CHCl_3$).

Typical procedure for epoxidation

To a vial with alkene **2** (1.18 mmol) were added 11 mL of CH_3CN and 7.6 mL of 4 × 10^{-4} M ethylenediaminetetraacetic acid in H_2O. The solution was cooled to 0 °C, and 1,1,1-trifluoroacetone (1.33 g, 11.9 mmol) was added. A mixture of solid Oxone^{TM} (3.63 g, 4.36 mmol) and $NaHCO_3$ (743 mg, 8.85 mmol) was added in four portions over 45 min. The reaction was stirred for 2 h at 0 °C, then diluted with 5 mL of H_2O, and extracted with CH_2Cl_2 (3 × 25 mL). The organic layers were combined and dried over anhydrous Na_2SO_4. Filtration and evaporation in vacuo furnished the crude product, which was purified by column chromatography (silica gel eluting with hexane/EtOAc) to provide epoxides **3a-j**. Compounds **3a-h** were identical in ^{1}H-NMR with *ent*-**3a-h** which were reported previously.[26]

(1a*S*,1b*R*,6*R*,6a*R*)-6-Dodecyltetrahydrooxireno[2',3':3,4]pyrrolo[1,2-c]oxazol-4(1*aH*)-one (3i).

80% yield; ^{1}H-NMR (400 MHz, $CDCl_3$) δ: 0.88 (3H, t, *J* = 6.8 Hz), 1.26-1.51 (22H, m), 3.55 (1H, d, *J* = 2.9 Hz), 3.61 (1H, d, *J* = 2.9 Hz), 3.98 (1H, dd, *J* = 3.7, 8.7 Hz), 4.04 (1H, dd, *J* = 4.8, 9.2 Hz), 4.47 (1H, t, *J* = 4.3 Hz), 4.55 (1H, dd, *J* = 9.2, 17.9 Hz). ^{13}C-NMR (100 MHz, $CDCl_3$) δ: 14.08, 22.64, 26.06, 29.29, 29.31, 29.41, 29.50, 29.59, 29.61, 30.01, 31.87, 55.26, 57.17, 58.70, 60.45, 64.63, 162.54. IR (neat) cm^{-1} : 1747, 2850, 2919. EI-MS (m/z) : 309 (M^+). HRMS Calcd. for $C_{18}H_{31}NO_3$: 309.2304, Found: 309.2309, $[\alpha]_D^{25}$ = -34.3 (*c* 0.35, $CHCl_3$).

(1a*S*,1b*R*,6*R*,6a*R*)-6-Tridecyltetrahydrooxireno[2',3':3,4]pyrrolo[1,2-c]oxazol-4(1*aH*)-one (3j).

80% yield; ^{1}H-NMR (400 MHz, $CDCl_3$) δ: 0.88 (3H, t, *J* = 7.2 Hz), 1.26-1.55 (24H, m), 3.55-3.61 (2H, m), 3.97-4.02 (2H, m), 4.48-4.53 (2H, m), ^{13}C-NMR (100 MHz, $CDCl_3$) δ: 14.10, 22.67, 26.08, 29.32, 29.33, 29.43, 29.51, 29.61, 29.66, 30.04, 31.89, 55.26, 57.19, 58.74, 60.46, 64.64, 162.54. IR (neat) cm^{-1} : 1757, 2850, 2918. EI-MS (m/z) : 323 (M^+). HRMS Calcd. for $C_{19}H_{33}NO_3$: 323.2460, Found : 323.2449, $[\alpha]_D^{19}$ = -26.2 (*c* 0.21, $CHCl_3$).

Typical Procedure for the preparation of a diol.

Trifluoroacetic acid (0.70 mL, 9.12 mmol) was added to a solution of the epoxide **3** (0.773 mmol) in THF/H_2O (3/2, 6.8 mL). After being stirred at 80 °C for 72 h, the reaction mixture was cooled to room temperature and concentrated. The product was purified by flash chromatography (silica gel, eluting with CH_2Cl_2/CH_3OH or Et_2O/CH_3OH) to yield *trans*-diols **4a-j**. Compounds **4a-h** were identical in ^{1}H-NMR with *ent*-**4a-h** which were reported previously.[26]

(5*R*,6*R*,7*R*,7a*R*)-6,7-Dihydroxy-5-dodecyltetrahydropyrrolo[1,2-c]oxazol-3(1*H*)-one (4i).

82% yield, ^{1}H-NMR (400 MHz, $CDCl_3$) δ: 0.88 (3H, t, *J* = 7.2 Hz), 1.26-1.67 (22H, m), 3.63-3.68 (1H, m), 3.83-3.97 (3H, m), 4.36 (1H, dd, *J* = 3.4, 9.2 Hz), 4.54 (1H, t, *J* = 8.7 Hz). ^{13}C-NMR (100 MHz, $CDCl_3$) δ: 14.10, 22.67, 26.19, 29.36, 29.50, 29.63, 29.68, 29.71, 29.73, 29.78, 29.91, 31.92, 33.02, 62.16, 65.35, 67.05, 80.80, 83.49, 162.73. IR (neat) cm^{-1} : 1717, 2850, 2919, 3379. EI-MS (m/z) : 327 (M^+). HRMS Calcd. for $C_{18}H_{33}NO_4$: 327.2410, Found : 327.2396, $[\alpha]_D^{25}$= -23.4 (*c* 0.29, $CHCl_3$).

(5*R*,6*R*,7*R*,7a*R*)-6,7-Dihydroxy-5-tridecyltetrahydropyrrolo[1,2-c]oxazol-3(1*H*)-one (4j).

99% yield, ^{1}H-NMR (400 MHz, $CDCl_3$) δ: 0.88 (3H, t, *J* = 6.8 Hz), 1.26-1.64 (24H, m), 3.49 (1H, brs), 3.85-3.93 (3H, m), 4.31-4.38 (1H, m), 4.46-4.54 (1H, m). ^{13}C-NMR (100 MHz, $CDCl_3$) δ: 14.09, 22.67, 26.13, 29.36, 29.46, 29.51, 29.62, 29.68, 29.73, 29.79, 29.91, 31.92, 32.90, 62.10, 65.20, 67.14, 80.72, 83.36, 162.86. IR (neat) cm^{-1} : 1727, 2851, 2919, 3447. EI-MS (m/z) : 341 (M^+). HRMS Calcd. for $C_{19}H_{35}NO_4$: 341.2566, Found : 341.2573, $[\alpha]_D^{23}$= -8.3 (*c* 0.33, $CHCl_3$).

Typical Procedure for hydrolysis.

NaOH (280 mg, 7.00 mmol) was added to a solution of diol **4** (230 mg, 0.674 mmol) in EtOH/H_2O (2:1, 8.4 mL), and the mixture was refluxed for 1 h. The reaction mixture was cooled to room temperature and concentrated. The product was purified by flash chromatography (silica gel, eluting with

Et_2O/MeOH/25% NH_3(aq) = 80/20/1 → 0/100/2) to yield iminosugars **5a-j**. Compounds **5a-h** were identical in ^{1}H-NMR with *ent*-**5a-h** which were reported previously.[26]

α-1-*C*-Butyl-DAB (5a).

90 % yield; $[\alpha]_D^{24}$ = +47.2 (*c* 0.80, CH_3OH). *Lit. ent*-**5a**[26] : $[\alpha]_D^{27}$ = -47.7 (*c* 1.00, CH_3OH).

α-1-*C*-Pentyl-DAB (5b).

47 % yield; $[\alpha]_D^{27}$ = +54.3 (*c* 0.82, CH_3OH). *Lit. ent*-**5b**[26] : $[\alpha]_D^{24}$ = -53.5 (*c* 1.44, CH_3OH).

α-1-*C*-Hexyl-DAB (5c).

58 % yield, $[\alpha]_D^{26}$ = +66.6 (*c* 0.32, CH_3OH). *Lit. ent*-**5c**[26] : $[\alpha]_D^{22}$ = -51.1 (*c* 1.18, CH_3OH).

α-1-*C*-Heptyl-DAB (5d).

67 % yield, $[\alpha]_D^{27}$ = +42.9 (*c* 1.33, CH_3OH). *Lit. ent*-**5d**[26] : $[\alpha]_D^{24}$ = -46.1 (*c* 1.00, CH_3OH).

α-1-*C*-Octyl-DAB (5e).

46% yield, $[\alpha]_D^{26}$ = +34.6 (*c* 0.17, CH_3OH). *Lit. ent*-**5e**[26] : $[\alpha]_D^{23}$ = -44.2 (*c* 0.70, CH_3OH).

α-1-*C*-Nonyl-DAB (5f).

47 % yield, $[\alpha]_D^{27}$= +41.2 (*c* 0.50, CH_3OH). *Lit. ent*-**5f**[26] : $[\alpha]_D^{23}$ = -45.5 (*c* 1.33, CH_3OH).

α-1-*C*-Decyl-DAB (5g).

68 % yield, $[\alpha]_D^{26}$= +36.1 (*c* 0.99, CH_3OH). *Lit. ent*-**5g**[26] : $[\alpha]_D^{22}$ = -36.5 (*c* 0.41, CH_3OH).

α-1-*C*-Undecyl-DAB (5h).

65% yield, $[\alpha]_D^{27}$ = +35.7 (*c* 0.72, CH_3OH). *Lit. ent*-**5h**[26] : $[\alpha]_D^{23}$ = -37.8 (*c* 1.00, CH_3OH).

α-1-*C*-Dodecyl-DAB (5i).

68% yield, ^{1}H-NMR (400 MHz, CD_3OD) *d*: 0.92 (3H, t, *J* = 7.2 Hz), 1.29-1.45 (23H, m), 1.70 (1H, brs), 2.91 (1H, dd, *J* = 7.7, 12.6 Hz), 3.04 (1H, dd, *J* = 6.3, 10.6 Hz), 3.58-3.63 (2H, m), 3.71 (1H, dd, *J* = 3.9, 11.6 Hz), 3.79 (1H, t, *J* = 6.8 Hz). ^{13}C-NMR (100 MHz, CD_3OD) *d*: 14.44, 23.73, 27.70, 30.48, 30.68, 30.73, 30.74, 30.76, 30.78, 30.80, 33.08, 34.97, 62.87, 64.55, 79.30, 83.29. IR (KBr) cm^{-1} : 2850, 2918, 3292. FAB-MS (m/z) : 302 (M^++1). HRMS Calcd. for $C_{17}H_{36}NO_3$: 302.2695, Found : 302.2693, $[\alpha]_D^{23}$ = +13.4 (*c* 0.25, CH_3OH).

α-1-*C*-Tridecyl-DAB (5j).

74% yield; ^{1}H-NMR (400 MHz, CD_3OD) *δ*: 0.92 (3H, t, *J* = 7.2 Hz), 1.29-1.59 (23H, m), 1.73-1.83 (1H, m), 3.03-3.08 (1H, m), 3.16-3.20 (1H, m), 3.64-3.77 (3H, m), 3.86 (1H, t, *J* = 6.3 Hz). ^{13}C-NMR (100 MHz, CD_3OD) *δ*: 14.45, 23.74, 27.60, 30.48, 30.65, 30.72, 30.75, 30.77, 30.80, 30.80, 33.08, 34.38, 62.20, 63.16, 64.78, 78.77, 82.70. IR (KBr) cm^{-1} : 2851, 2919, 3294. EI-MS (m/z) : 315 (M^+). HRMS Calcd. for $C_{18}H_{37}NO_3$: 315.2773, Found : 315.2773, $[\alpha]_D^{22}$ = +59.7 (*c* 0.12, CH_3OH).

Enzyme assay

Brush border membranes were prepared from the rat small intestine according to the method of Kessler *et al.*,[29] and were assayed at pH 6.8 for rat intestinal maltase and sucrase using the appropriate disaccharide as substrate. The reaction mixture contained 25 mM substrate and the appropriate amount of enzyme, and the incubations were performed for 10-30 min at 37 ˚C. The reaction was stopped by heating at 100 ˚C for 3 min. After centrifugation (600 g; 10 min), 0.05 mL of the resulting reaction mixture were added to 3 mL of the Glucose CII-test Wako (Wako Pure Chemical Ind., Osaka, Japan). The absorbance at 505 nm was measured to determine the amount of the released D-glucose. The inhibitory activity toward β-glucocerebrosidase was measured with Cerezyme (Genzyme ; Boston, MA) as the enzyme source and 4-methylumbelliferyl-β-D-glucopyranoside (Sigma-Aldrich Co ; St. Louis, Mo, USA) as substrate. The reaction mixture consisted 100 mM McIlvaine buffer (pH 5.2), 0.25% sodium taurocholate and 0.1% Triton X-100 (Nacalai Tesque Inc ; Kyoto, Japan), and the appropriate amount of enzyme. The reaction mixture was pre-incubated at 0˚C for 45 min, and the reaction was started by the using 3 mM substrate solution, followed by incubation at 37˚C for 30 min. The reaction was stopped by the addition of 1.6 mL of the solution of 400 mM glycine-NaOH solution (pH 10.6). The released 4-methylumbelliferone was measured (excitation 362 nm, emission 450 nm) with a F-4500 fluorescence spectrophotometer (Hitachi, Tokyo, Japan). Kinetic parameters were determined by the double-reciprocal plot method of Lineweaver-Burk plots at increasing substrate concentrations.

Thermostability of β-glucocerebrosidase

The enzyme β-glucocerebrosidase was incubated at 45 ˚C in 100 mM McIlvaine buffer (pH 5.2) containing 0.25% sodium taurocholate and 0.1% Triton X-100 for 0, 20, 40, and 60 min. After incubation, the remaining β-glucocerebrosidase activity was assayed immediately using 3 mM 4-methylumbelliferyl-β-D-glucopyranoside as substrate. The values were expressed as relative to the activity before the incubation (100%). Time zero points correspond to the conditions that reaction mixtures were not heat-treated and kept on ice for the duration of the heat inactivation experiment.

Pharmacological chaperone activity

The Gaucher's cell line with β-glucocerebrosidase mutation of N307S (GM00372) was obtained from the Coriell Cell Repositories (Camden, NJ). The Gaucher N307S fibroblasts were cultured in EMEM (Eagle's Minimum Essential Medium; Sigma-Aldrich Co) supplemented with 15% FCS. Cells were cultured in a water-jacket incubator at 37˚C under 5 % CO_2 in the presence or absence of samples for 6 days. After washing twice with a medium, the cell pellet were homogenized in a citrate buffer (pH 5.2) containing 0.25% sodium taurochole and 0.1% Triton X-100. The supernatant obtained from the homogenate after centrifugation at 1,000 g for 5 min was

subject to enzyme assays and protein determination. Intercellular β-glucocerebrosidase activities were determined with 4-methylumbelliferyl-β-D-glucoside as substrate at pH 5.2.

Immunocytochemistry

The Gaucher's cell line with β-glucocerebrosidase mutation of N307S (GM00372) were treated with rabbit polyclonal anti-GCase serum as a primary antibody for the detection of GCase (GeneTex, San Francisco, CA), and monoclonal anti-LAMP-1 serum (abcam plc., Cambridge, UK) for the detection of lysosomes. Hilyte Fluor^{TM}488-conjugated goat anti-rabbit IgG serum and Fluor^{TM}594-conjugated goat anti-mouse IgG serum (both from AnaSpec, Inc., Fremont, CA) were used as secondary antibodies. Gaucher fibroblasts (2.5×10^4 cells) were grown on sterile coverslips with presence or absence of iminosugars and cultured with 6 days in EMEM. All immunocytochemistry procedures were performed at room temperature. After cells had been washed three times with PBS, they were fixed with 1 mL of 4% paraformaldehyde in PBS for 15 min, and then washed three times with PBS. The cells were permeated with 1 mL of 0.01% Triton X-100 in PBS for 15 min, and then washed three times with PBS. After a 30 min treatment with 1 mL of blocking solution (5% skim milk in PBS), the cells were incubated with the primary antibody diluted in 1% skim milk in PBS for 30 min, and this was followed by three washes with 1 mL of PBS. Coverslips were then incubated in the dark with the secondary antibody diluted in 1% skim milk in PBS for 30 min, and this was followed by three washes with 1 mL of PBS. The coverslips were mounted with a drop of Vectashield mounting medium (Vector Laboratories, Inc., Burlingame, CA), and fluorescence was visualized using an Olympus fluorescence microscope (Olympus, Tokyo, Japan).

Docking studies

The crystal structure of human β-glucocerebrosidase complex with D-isofagomine (PDB code: 2NSX) was used for the docking analysis of α-1-*C*-tridecyl-DAB (**5j**); this crystal structure was determined under acidic conditions (pH4.5) reflecting the lysosome acidic environment.[30] The comparison between the B chain and D chain in the crystal structure about the binding site around a ligand suggested that the side chain of Asn396 is flexible. We therefore employed Induced Fit protocol (Schrödinger Suite 2009, Schrödinger, LLC) that allows both structures of a ligand and a protein to move.[31] Water molecules were removed from the crystal structure and hydrogen atoms were added. The 3D structures of α-1-C-tridecyl-DAB (**5j**) were generated using LigPrep and ConfGen (Schrodinger suite 2009). Standard-precision mode was used in the docking analysis. For a first docking step of the Induced Fit protocol, the van der Waals radii scaling for the ligand and the protein were reduced to 0.5 and 0.7 respectively. Asn396 was mutated to alanine temporarily. In a second step, Ala396 was restored to Asn396 and residues within 5 Å around a docked ligand were refined so that their side chains became optimal. In a final step, the ligand was docked again into induced-fit receptor structures and the output poses were ranked based on IFD score. The top1 pose ranked by IFDscore was selected as the complex structure of α-1-*C*-tridecyl-DAB with β-glucocerebrosidase.

Acknowledgment

This work was supported in part by a Grant-in-Aid for Scientific Research (C) (No: 26460143) (AK) from the Japanese Society for the Promotion of Science (JSPS) and a Leverhulme research fellowship (GWJF).

References

1 R. O. Brady, J. N. Kanfer, D. Shapiro, *Biochem. Biophys. Res. Commun*., **1965**, *18*, 221-225.
2 T. D. Butters, *Curr. Opin. Chem. Biol.*, **2007**, *11*, 412-418.
3 M. Horowitz, A. Zimran, Hum. Mutat. **1994**, *3*, 1-11.
4 M. Horowitz, S. Wilder, Z. Horowitz, O. Reiner, T. Gelbart, E. Beutler, *Genomics*, **1989**, *4*, 87.
5 E. Sidransky, *Mol. Genet. Metab*., **2004**, *83*, 6-15.
6 R. R. Wei, H. Hughes, S. Boucher, J. J. Bird, N. Guziewicz, S. M. Van Patten, H. Qiu, C. Q. Pan, T. Edmunds, *J. Biol. Chem.*, **2011**, *286*, 299-308.
7 S. Ishii, R. Kase, H. Sakuraba, Y. Suzuki, *Biochem. Biophys. Res. Commun*., **1993**, *197*, 1585-1589.
8 R. Kase, U. Bierfreund, A. Klein, T. Kolter, K. Utsumi, K. Itoh, K. Sandhoff, H. Sakuraba, *Biochim. Biopys. Acta*. **2000**, *1501*, 227-235.
9 A. R. Sawkar, S. L. Adamski-Werner, W.-C. Cheng, C.-H. Wong, E. Beutler, K.-P. Zimmer, J. W. Kelly, *Chem. Biol*. **2005**, *12*, 1235-1244.
10 J.-Q. Fan, S. Ishii, N. Asano, Y. Suzuki, *Nat. Med*. **1999**, *5*, 112-115.
11 A. R. Sawker, W. -C. Cheng, E. Beautler, C. –H. Wong, W. E. Baich, J. W. Kelly, *Proc. Natl. Acad. Sci. U.S.A*., **2002**, *99*, 15428-15433.
12 G. M. Pastores, N. L. Barnett, E. H. Kolodny, *Clin. Ther*. **2005**, *27*, 1215-1227.
13 H. R. Mellor, F. M. Platt, R. A. Dwek, T. D. Butters, *Biochem. J*. **2003**, *374*, 307-314.
14 R. E. Boyd, G. Lee, P. Rybczynski, E. R. Benjamin, R. Khanna, B. A. Wustman, K. J. Valenzano, *J. Med. Chem.* **2013**, *56*, 2705-2725.
15 X. Zhu, K. A. Sheth, S. Li, H. H. Chang, J. –Q. Fan, *Angew. Chem. Int. Ed. Engl*. **2005**, *44*, 7450-7453.
16 L. Yu, K. Ikeda, A. Kato, I. Adachi, G. Godin, P. Compain, O. Maryin, N. Asano, *Bioorg. Med. Chem*., **2006**, *14*, 7736-7744.
17 M. Aguilar-Moncayo, M. I. García-Moreno, A. Trapero, M. Egido-Gabás, A. Llebaria, J. M. García Fernández and C. Ortiz Mellet, *Org. Biomol. Chem.*, **2011**, *9,* 3698-3713.
18 H.-H. Chang, N. Asano, S. Ishii, Y. Ichikawa, J.-Q. Fan, *FEBS J.* **2006**, *273*, 4082-92.
19 Z. Yu, A. R. Sawkar, L. J. Whalen, C. H. Wong, J. W. Kelly, *J. Med. Chem.* **2007**, *50*, 94-100.
20 P. Compain, O. R. Martin, C. Boucheron, G. Godin, L. Yu, K. Ikeda, N. Asano, *ChemBioChem*, **2006**, *7*, 1356-1359.
21 F. Oulaidi, S. Front-Deschamps, E. Gallienne, E. Lesellier, K. Ikeda, N. Asano, P. Compain, O. R. Maryin, C*hemBioChem*, **2011**, *6*, 353-361.
22 E. D. Goddard-Borger, M. B. Tropak, S. Yonekawa, C. Tysoe, D. J. Mahuran, S. G. Withers, *J. Med.Chem*. **2012**, *55*, 2737-2745.
23 Y. Minami, C. Kuriyama, K. Ikeda, A. Kato, K. Takebayashi, I. Adachi, G. W. J. Fleet, A. Kettawan, T. Okamoto, N. Asano, *Bioorg. Med. Chem.* **2008**, *16*, 2734-2740.

24 B. J. Ayers, N. Ngo, S. F. Jenkinson, R, F. Martines, Y. Shimada, I. Adachi, A. C. Weymouth-Wilson, A. Kato, G. W. J. Fleet, *J. Org. Chem*. **2012**, *77*, 7777-7792.
25 Y. Natori, T. Imahori, K. Murakami, Y. Yoshimura, S. Nakagawa, A. Kato, I. Adachi, H. Takahata, *Bioorg. Med. Chem. Lett.* **2011**, *21*, 738-741.
26 A. Kato, E. Hayashi, S. Miyauchi, I. Adachi, T. Imahori, Y. Natori, Y. Yoshimura, R. J. Nash, H. Shimaoka, I. Nakagome, J. Koseki, S. Hirono, H. Takahata, *J. Med. Chem*. **2012**, *55*, 10347-10362.
27 S. F. Jenkinson, D. Best, A. W. Saville, R. F. Martinez, S. Nakagawa, T. Kunimatsu, D. S. Alonzi, T. D. Butters, C. Norez, F. Becq, Y. Blériot, F. X. Wilson, A. C. Weymouth-Wilson, A. Kato, G. W. J. Fleet, *J. Org. Chem*. **2013**, *78*, 7380-7397.
28 A. Kato, I. Nakagome, S. Nakagawa, Y. Koike, R. J. Nash, I. Adachi, S. Hirono, *Bioorg. Med. Chem.* **2014**, *22*, 2435-2441.
29 M. Kessler, O. Acuto, C. Strelli, H. Murer, G. A. A. Semenza, *Biochem. Biophys. Acta* **1978**, *506*, 136-154.
30 R. L. Lieberman, B. A. Wustman, P. Huertas, A. C. Powe, Jr, C. W. Pine, R. Khanna, M. G. Schlossmacher, D. Ringe, G. A. Petsko, *Nat Chem Biol* **2007,** *3*, 101-107
31 W. Sherman, T. Day, M. P. Jacobson, R.A. Friesner, R. Farid, *J. Med. Chem.* **2006**, *49*, 534-553.